Oxidation Modification of Fuorinated Graphite and Its Reaction Mechanism

Hao Li (376467729lihao@163.com)
Xi'an Research Institute of High-Tech
Song Bi
Xi'an Research Institute of High-Tech
Xiaojing Yuan
Xi'an Research Institute of High-Tech
Zhaohui Liu
Xi'an Research Institute of High-Tech
Yongzhi Song
Xi'an Research Institute of High-Tech
Jinjin Wang
Xi'an Research Institute of High-Tech
Genliang Hou
Xi'an Research Institute of High-Tech

Research Article

Keywords: Oxidized fluorinated graphite, Hummers method, modification mechanism, fluorocarbon bond activation

Posted Date: October 4th, 2021

DOI: https://doi.org/10.21203/rs.3.rs-943586/v1

Abstract

In this paper, Hummers method was used to oxidize fluorinated graphite in order to study the modification mechanism. The chemical composition and microstructure of the products before and after the reaction were characterized and analyzed. Oxidized fluorinated graphite (OFG) obtained by oxidation has a thin layered structure and different oxygen content. The main mechanism of $KMnO_4$ modification is that MnO_3^+ with Lewis acid property can catalyze the activation of the fluorocarbon bond, which breaks to form F ion. At the same time, the unsaturated carbon bond is oxidized, resulting in the increase of carbon oxygen bond content and the generation of some OFG nano fragments. With the increase in $KMnO_4$ dosage, the fluorocarbon bond will be gradually catalyzed to react according to its activity while the unsaturated carbon bond is oxidized, finally there are still some isolated fluorocarbon bonds with weak activity.

1 Introduction

Fluorinated graphene (FG) is grafted with F atom on the graphene skeleton, while graphene oxide (GO) is grafted with oxygen-containing groups (carboxyl, epoxy, carbonyl, etc.) on the graphene. The substance grafted with fluorine atom and oxygen-containing group on the graphene is called fluorinated graphene oxide (OFG) or oxidized fluorinated graphite (OFG). OFG owns partial structure of GO and FG at the same time, and its performance is between them. By adjusting the content of F and O, the properties of OFG can be adjusted to a great extent, such as hydrophobicity [1], insulation [2], lubricity [3], photoelectric performance [4], etc. OFG does not have a relatively fixed property, but shows different properties according to the proportion of F and O, which has attracted great attention of researchers. For the preparation and application of OFG, many scholars have done useful exploration.

OFG is widely used in hydrophobic coatings [5, 6], sensors [7, 8], medicine [9, 10], photoelectric properties [11, 12] and many other aspects due to its unique performance adjustment space. OFG was added into 2.5wt% PDMS toluene solutions, taking TEOS as coupling agent and dibutyltin dilaurate as catalyst, after mixing, the coated film was found that the higher the OFG content, the better the hydrophobicity. When content of OFG reached 60.2wt%, the contact angle was 173.7 ° and the rolling angle was 4 ° [5]. OFG synthesized by hydrothermal method was used to detect NH_3, whose limit concentration was 6.12ppb, 20 times higher than that of RGO [7]. Water-soluble OFG with nanometer size has good fluorescence, high near-infrared absorption and pH response, and can be used as drug delivery carrier [10]. OFG was prepared by Hummers method, and 4,4'-diaminodiphenyl ether (ODA) was grafted on it, then OFG-ODA/PI mixture can reduce the dielectric constant, and the content of 1 wt% was the best, whose Young's modulus was increased by 50% [12].

According to the raw materials, preparation of OFG can be roughly divided into two kinds. One is to prepare OFG with fluorinated graphite (FGi) as raw material by oxygen doping [5, 9, 13]. Mathkar used Hummers method to oxidize FGi of $(CF_{0.25})_n$, and adopted the method of solution separation to obtain high fluorine content OFG (HOFG) with good hydrophobicity and low fluorine content OFG dissolved in

water [1]. In addition, FGi was modified by molten KOH and NaOH mixture to obtain OFG quantum dots (about 3nm), which have stable fluorescence and can be applied in different pH [14]. The heating method of FGi(F/C=1)/DMF solution was also utilized to prepare OFG [6]. Beyond that, the other is to use GO as raw material, and take HF, XeF_2, HPF_6, etc. as fluorinating agents, so as to obtain OFG [15, 16, 17]. GO was fluorinated by HNO_3/HF hydrothermal method to obtain OFG with F and O content of 21.5 at% and 14.2 at% respectively, which had good dispersion in water [15]. XeF_2 was used to obtain OFG with F content of 28.6 at% [16]. OFG was also prepared by using HPF_6 to fluorinate GO, which detected histamine with a sensitivity of about 7 nM [17].

In general, there are many researches on the preparation and application of OFG. The cost of oxidation modification of FGi is low and the experimental conditions are simple, so there are relatively more researches in this field. However, there are still some problems that can't control the content of F and O, and the reaction mechanism of FGi oxidation is not very clear, which makes it difficult to control the reaction accurately. In view of this, FGi was used as the material to obtain OFG with different content of fluorine and oxygen by controlling reacting conditions, and the reaction mechanism was explored by studying the reaction processes and products.

2 Experimental Section

2.1 Materials Preparation

FGi with a fluorine content of ~42 wt%, ~60 wt% and ~65 wt% was provided by Shanghai CarFluor Ltd. Concentrated sulphuric acid (H_2SO_4), potassium permanganate ($KMnO_4$), concentrated hydrochloric acid (HCl), potassium hydroxide (KOH), ethanol (CH_3CH_2OH), hydrogen peroxide (H_2O_2), etc. was provided from Sinopharm Chemical Reagent Co., Ltd. Deionized water (>18MΩ.cm) was used for rinsing and as the solvent as well.

2.2 Synthesis of OFG

The modified Hummers method was utilized to prepare OFG [18]. The detailed steps were as follows: 1 g FGi was added into 80 ml concentrated H_2SO_4 and stirred in an ice-water bath at 0 ℃ for 10min, then 8 g $KMnO_4$ was added very slowly while stirring. After two hours' ice-water bath reaction, the solution went on two hours' 40°C water baths. After a water bath ultrasonication for 20 min (500W, 45/80kHz alternating for 40 s), excess H_2O_2 was added to the solution turning the purplish red solution to transparency (removing the unreacted $KMnO_4$). The solution was filtered by suction (0.22 μm PTFE hydrophilic filter membrane). The solid obtained was washed with water and ethanol for many times, then filtered by suction. Finally, the sample was dried at 100 ℃ after freeze-drying, and the product was marked as OFG42-1. Based on the preparation of OFG42-1, $KMnO_4$ was changed to 2 g, which was recorded as OFG42-2. FGi 42 wt% and $KMnO_4$ were changed to 2 g and 3 g, and the product was OFG42-3. The corresponding product of 3 g FGi 42 wt% and 3 g $KMnO_4$ was OFG42-4.

2.3 Separation and extraction of residual products

After the separation of OFG, Mn^{2+}, H^+, SO_4^{2-}, K^+, MnO_4^-, H_2O and possible fluorine-containing substances may exist in the solution. Excessive H_2O_2 will reduce MnO_4^- to Mn^{2+}. Add excessive KOH to adjust the solution to pH=9.5, so that the existing Mn^{2+} can be completely converted into the precipitate. Then, the whole solution were filtered by suction with 0.2 μm hydrophilic PTFE membrane, and obtained precipitate was added water into and filtered into many times to remove K_2SO_4. The final product was labeled P (precipitate), for example, the precipitate corresponding to OFG42-1 was P42-1. The remaining solution after the first filtration still contains saturated K_2SO_4. If it is dried directly, the content of fluorine-containing substances will be very low and difficult to detect. Therefore, firstly it is concentrated to 100 ml and then frozen in a 0 ℃ ice water bath for 1 h, so as to reduce the solubility of K_2SO_4 and make it precipitate more. The filtrate was dried at 140 ℃ for at least 48 hours, and the product was labeled as RP (reaction product), for example, the reaction product corresponding to OFG42-1 was RP42-1.

2.4 Characterization

Fourier transform infrared spectra (FT-IR) from 400 cm^{-1} to 4000 cm^{-1} were recorded by a VERTEX70 spectrometer (Bruker, Germany). X-ray photoelectron spectroscopic (XPS) analysis was carried out on an X-ray photoelectron spectrometer (Thermo Fisher Scientific, USA) with monochromatic Al Kα (1486.6ev) line. All the binding energies were calibrated using 284.6 eV of C 1s. The characterization of crystal structure was implemented on an X-ray diffractometer with the excitation source of Ka line of Cu target (λ = 0.154nm) (X'Pert PRO, PAnalytical, Netherlands). The micromorphology was observed by VEGA2XMU scanning electron microscope (SEM, TESCAN, Czechoslovakia), and the products were directly adhered to the conductive carbon belt for gold spraying. The element distribution was measured by Oxford 7718 (EDS, Oxford, UK) equipped with SEM. F ion content was detected by ion chromatograph (Thermo Fisher, ICS-1000 type, USA).

3 Results And Discussion

3.1 Morphology and Chemical Composition of OFG

After the modification of different amount of $KMnO_4$, FT-IR spectra of OFG42 are shown in Fig. 1. OFG42-1, OFG42-2, OFG42-3 and OFG42-4 is respectively corresponding to FGi 42 wt%/$KMnO_4$ of 1g / 8g, 1g / 2g, 2g / 3g and 3g / 3g. Different from FGi 42 wt% owning only C-F bond stretching vibration peak at 1186cm^{-1} [19, 20], there are many kinds of oxygen-containing groups from OFG42-1 to OFG42-4: stretching vibration peaks of -OH, C=O and C-O are respectively at 3436cm^{-1}, 1728cm^{-1} and 1039cm^{-1}, 1392cm^{-1} is corresponding to C-OH bending vibration peaks. In addition to the introduction of oxygen-containing groups, the peak position of C-F shifts from 1176 cm^{-1} to 1220 cm^{-1}. The peak at 1573 cm^{-1} belongs to the A_{2u} vibration mode of graphite phase [18]. From OFG42-1 to OFG42-4, with the decrease of $KMnO_4$ content, the strength of -OH stretching vibration peak and bending vibration peak of adsorbed

water decreased obviously, indicating the decrease of adsorbed water content, which is related to the content of C-OH, to a certain extent, indicating the decrease of C-OH content. Different from other OFG, the peak of OFG42-4 at 1573 cm^{-1} is very obvious, which shows that when the mass ratio of $KMnO_4$/FGi 42wt% is 1, the amount of $KMnO_4$ is insufficient, resulting in the existence of a part of graphite phase can't be oxidized. FT-IR results showed that with the decrease of $KMnO_4$ content, the number of oxygen-containing groups decreased gradually, and the unoxidized graphite phase appeared.

Figure 2 shows the XPS spectra of OFG, mainly including C, O and F. There are obvious O1s peaks from OFG42-1 to OFG42-4, while the F1s peak is weakened, and the F1s peak of OFG42-1 and OFG42-2 is significantly reduced. The content of O and F is shown in Table 1. When the mass ratio of $KMnO_4$/FGi 42wt% is 2 and 8, the content of F and O is close, indicating that excessive $KMnO_4$ makes the oxidation complete at this moment and some of the fluorocarbon bonds are relatively stable, which is difficult to remove due to strong oxidation. When the mass ratio is lower than 2, the O content of OFG42-3 and OFG42-4 decreases obviously. Both of them are about 20 at%, and the F content is also about 20 at%. This shows that with the decrease of $KMnO_4$ content, those unsaturated carbon bonds can't be oxidized, and a large number of fluorocarbon bonds have not been destroyed, so the F content is well maintained. A small amount of S element may come from sulfate impurity. Fig. S1 shows the distribution of C, O and F elements in OFG42-1, OFG42-2, OFG42-3 and OFG42-4 in the supporting information. The element distribution of O and F is basically the same as that of C, indicating that the distribution of O and F is uniform.

Table 1
Element content of OFG42-1, OFG42-2, OFG42-3 and OFG42-4

Product	C (at%)	O (at%)	F (at%)	Other (at%)
FGi 42 wt%	67.4	0.9	31.7	
OFG42-1	64.5	28.5	6	S 1.0
OFG42-2	64.8	29.3	4.8	S 1.1
OFG42-3	56.5	20.3	21.6	S 1.6
OFG42-4	61.9	19.8	17.3	S 1.0

High-resolution C1s spectra of OFG are shown in Fig. 3. There are a lot of carbon oxygen bonds in the OFG at 286.3 eV ~ 288.9 eV of C1s, but the content of fluorocarbon bonds is obviously reduced. Table 2 shows the composition of the carbon bond in C1s peak. From OFG42-1 to OFG42-4, the content of sp^2 C=C bond and fluorocarbon bond is lower than FGi 42 wt%, while the content of sp^3 C-C bond and carbon oxygen bond is higher. This shows that the fluorocarbon bond and sp^2 C=C bond is destroyed and becomes the carbon oxygen bond in the oxidation process. According to F1s peak and FT-IR results, ~ 288.6 eV in the OFG42-1 and OFG42-2 belongs to O-C=O bond, while it belongs to semi ion C-F bond in the OFG42-3 and OFG42-4 [21, 22].

Table 2
Location, ascription and content of carbon-containing groups in OFG42-1, OFG42-2, OFG42-3 and OFG42-4

Product	sp^2 C=C 284.6eV	sp^3 C-C 285.3eV	C-O 287.0eV	C=O 287.9eV	O-C=O/semi ionic C-F 288.6eV	C-F 289.8eV	$-CF_2$ 291.7eV
FGi 42 wt%	38.7%	13.2%	4.3%		3.5%	36.2%	4.1%
OFG42-1	9.4%	32.2%	2.7%	37.0%	9.4%	9.3%	
OFG42-2	7.1%	29.2%	10.1%	36.7%	6.9%	9.9%	
OFG42-3	6.6%	24.4%	33.3%	3.9%	2.1%	27.9%	1.8%
OFG42-4	23.1%	16.8%	34.1%		4.3%	20.3%	1.6%

With the mass ratio increasing, the content of carbon oxygen bond increases gradually. There are more sp^2 C=C bonds in OFG42-4, and only C-O bonds. When the mass ratio is 1.5, sp^2 C=C bond content of OFG42-3 decreases greatly, and C=O bond begins to appear. When the mass ratio is 2, the carboxyl group also begins to appear, and at this time, $KMnO_4$ amount goes on increasing, but only part of the C-O bond is converted to ketone or carboxyl group, and the total amount of carbon oxygen bond is no longer increased, indicating that when the mass ratio is 2, the amount of $KMnO_4$ is enough to oxidize the unsaturated carbon-carbon bond. In general, the decrease of fluorocarbon bond content is consistent with the increase of carbon oxygen bond content. Oddly, the amount of $KMnO_4$ in OFG42-4 is insufficient, while its fluorocarbon bond content is lower than that of OFG42-3 with more $KMnO_4$, and indicating the whole oxidation system in OFG42-4 is more inclined to activate the fluorocarbon bond to make it react, rather than to oxidize the unsaturated carbon bond, whose possible reason will be explained below. When the mass ratio is 8, there is still a part of C-F bond, which indicates that even if $KMnO_4$ is excessive, some of the fluorocarbon bond can't be activated.

Fig. 4 shows high-resolution F1s spectra of OFG. 687.4 eV, 688.5 eV and 689.3 eV are corresponding to semi ion C-F bond, C-F covalent bond and $-CF_2$ bond respectively. When the amount of $KMnO_4$ is enough, OFG42-1 and OFG42-2 have only C-F bond, and the content of F is less. When the amount of $KMnO_4$ is insufficient, similar to FGi 42 wt%, OFG42-3 and OFG42-4 own semi ion C-F bond, C-F covalent bond and $-CF_2$ bond.

Figure 5 is XRD spectra of OFG. After oxidation modification, the graphite phase corresponding to (002) diffraction peak basically disappeared. When the mass ratio is 1, the corresponding layer spacing of OFG42-4 diffraction peak at ~ 11.8 ° is 7.47 Å, which is larger than that of FGi 42wt%, and the weak shoulder peak nearby may belong to the stacked fluorocarbon bond structure. When the mass ratio is 1.5, the layer spacing of OFG42-3 increases to 8.83 Å, which indicates that the oxidation is more complete

and the layer spacing is larger. The diffraction peak of OFG42-2 is ~ 11.3 °, and the layer spacing is reduced to 7.8 Å, it may be that the fluorocarbon structure has been destroyed and most of it has changed into GO, which makes the layer spacing smaller. The shoulder peak at ~ 14.5 ° may belong to the residual fluorocarbon structure. When the mass ratio increases to 8, OFG42-1 basically has no change compared with OFG42-2.

The micro morphology of OFG is shown in Fig. 6. OFG42-1 to OFG42-4 shows a very thin layered structure, which indicates that the layered structure peels off well during the oxidation process, forming a single layer or several layers structure. OFG42-1 is the thinnest with many small fragments, while OFG42-4 with the least amount of $KMnO_4$ is thicker. The more $KMnO_4$ content, the better oxidation effect, the better stripping effect and the thinner layered structure.

In summary, FGi 42 wt% can be oxidized in different degrees by adjusting the mass ratio of $KMnO_4$/FGi 42 wt%. With the increase in mass ratio, the oxygen content is higher and sp^2 C=C is oxidized to C-O bond, then becomes C=O bonds, which is accompanied by the decrease of F content and C-F bonds. When the mass ratio is reduced to 1.5, OFG42-3 has a high content of fluorine and oxygen, 21.6 at% and 20.3 at% respectively. OFG obtained by oxidation has a thin layered structure, and oxidation intercalation results in the enlargement of the layer spacing, which makes it separate.

Like FGi 42wt%, reaction products of FGi 65wt% and FGi 60wt% is analyzed in the second part of the supporting information. From Fig. S2-S9 and Table S1-S3, it is found that FGi 65wt% and FGi 60wt% can't basically be oxidized by the solution of sulphuric acid and $KMnO_4$.

3.2 Chemical composition of residual products

Mn^{2+} will be produced after the reaction of sulphuric acid + $KMnO_4$ oxidation reaction, and precipitate will be produced after KOH treatment. Fig. 7 is FT-IR spectra of the precipitate P42-1. 517 cm^{-1} characteristic peak corresponds to the Mn-O bond. The narrow and sharp O-H peak of 3435 cm^{-1} indicates the existence of a large number of hydroxyl groups. 1626 cm^{-1} may be - OH bending vibration peak [23], and C-O stretching vibration peak is at 1025 cm^{-1}. There are Mn-O bonds and hydroxyl groups in P42-1. Mn^{2+} forms $Mn(OH)_2$ in alkaline solution, but $Mn(OH)_2$ is very unstable and easily oxidized to form $MnO(OH)_2$. Therefore, Mn may exist in the form of $MnO(OH)_2$.

XPS spectra of P42-1 is presented in Fig. 8, mainly including C, O, Mn. In addition, there is a small amount of S and F. S comes from the undeleted sulfate impurities, and F comes from FGi. High-resolution C1s spectra of precipitation is illustrated in Fig. 9. There is mainly C-O bond (~ 286.7 eV), O-C = O bond (~ 288.5 eV) and C-F bond (~ 289.6 eV), indicating that OFG also exists in P42-1 precipitation. This part of OFG should come from the oxidation fracture of an unsaturated carbon skeleton to small fragments. Because this part of OFG fragments is too small, 0.22 μm filter membrane can't filter it out during the first separation of OFG, and it remains in the filtrate. Then $MnO(OH)_2$ generated by adding KOH has certain flocculation and adsorption effect in the aqueous solution [24], so that OFG can't be dispersed into the

water. Combined with the results of FTIR and XPS, Mn mainly exists in the form of $MnO(OH)_2$. Similar to this, other precipitates are mainly composed of $MnO(OH)_2$ and some OFG.

Fig. 10 is FT-IR spectra of residual products RP42-1 to RP42-4. All have strong sulfate vibration peaks (1190 cm^{-1}, 1105 cm^{-1} and 616 cm^{-1}), and RP42-4 has silicate vibration peaks (870 cm^{-1} and 450 cm^{-1}). As shown in Fig. 11, XPS spectra mainly includes O, C, S, K and Na. Combined with FT-IR analysis, Na comes from the sodium silicate formed by the reaction of KOH and glass. O, S and K exist in the form of potassium sulfate. C is coming from FGi.

High-resolution C1s spectra of the remaining products RP42-1 to RP42-4 is shown in Fig. 12. There are mainly sp^2 C=C bond, sp^3 C-C bond and O-C=O bond. There are O-C=O bond and no fluorocarbon bond in all products, and C=O exists in some products, indicating that there is no OFG, and the C element in filtrate should exist in the form of GO. This part of GO also comes from the partial oxidation fracture in FGi, because its diameter is much smaller than that of OFG, and can't be filtered out and left in the solution. RP42-1, RP42-3 and RP42-4 are the same, basically without carbon oxygen bond, while RP42-2 has a large number of O-C=O bonds, which belong to GO. The above results show that there are small fragments of GO in RP42-1 to RP42-4. F1s peak is illustrated in Fig. 13, and the results are different. RP42-1 is suspected to have a peak of C-F bond in 688.8ev, but it is very weak, and the corresponding C-F bond in C1s is also difficult to distinguish, indicating that RP42-1 may have very small amount of OFG. The peak of RP42-2 at 684.7 eV belongs to the F ion bond [25, 26], and the F1s of RP42-3 and RP42-4 does not have any peak, but F ion is detected in the ion chromatography, indicating that the content of F is too small, which is beyond the detection range of XPS. In conclusion, there are F ions in the remaining products.

3.3 Reaction Mechanism

According to above analysis, FGi 42wt% can be oxidized by $KMnO_4$ +H_2SO_4 oxidation system and OFG with different F and O content is obtained. With the increase in the mass ratio of $KMnO_4$/FGi 42wt%, the degree of oxidation is deepening, and C-F bond can be activated to react, then turns into F ion. In order to study the whereabouts of F element in the reaction, Table 3 lists the F content of all products before and after reaction. F ions are detected in all the remaining products, indicating that some of the fluorocarbon bonds react after activation, but the amount is very small. F content of OFG42, P42 and RP42 is lower than that of raw materials, which indicated that in addition to the F converted into ionic bond, some F elements were separated from the reaction system in other forms.

Table 3
F content of all products before and after modification

Raw material	OFG	F content	P	F content	RP	F ion content
420 mg	OFG42-1	100 mg	P42-7	59.7 mg	RP42-1	1.9 mg
420 mg	OFG42-2	139.4 mg	P42-8	66.3 mg	RP42-2	3.0 mg
840 mg	OFG42-3	720 mg	P42-9	20.4 mg	RP42-3	0.6 mg
1260 mg	OFG42-4	982 mg	P42-10	18.3 mg	RP42-4	1.2 mg

Due to the chemical stability of the fluorocarbon bond, the activation of the fluorocarbon bond is difficult under normal conditions. Generally, catalytic agent is needed, and there is some selectivity for the reaction substrate. The fluorocarbon bonds of more active fluoroaromatics and fluoroalkenes are relatively easy to be activated, while the fluorocarbon bonds on the alkyl are difficult to be selectively activated [27]. Transition metals and their compounds are often used to catalyze C-F bond activation, such as rhodium, palladium, iridium copper, nickel, etc [28]. When $KMnO_4$ oxidizes FGi, Mn_2O_7 is generated and further reacts with sulphuric acid to generate MnO_3^+ [29, 30].

$$2KMnO_4 + 2H_2SO_4 \longrightarrow Mn_2O_7 + H_2O + 2KHSO_4$$

$$Mn_2O_7 + 2H_2SO_4 \longrightarrow 2MnO_3^+ + 2HSO_4^- + H_2O$$

The formed MnO_3^+ has strong Lewis acid, which can effectively promote the activation of fluorocarbon bond in aliphatic organic fluoride [31, 32]. The reason lies in the strong binding ability of fluorine in alkyl fluoride and metal center of Lewis acid, which can capture fluorine and promote the fracture of fluorocarbon bond. So the probable reaction principle of C-F bond activation is proposed in Fig. 14. In addition to oxidation of unsaturated carbon bonds, MnO_3^+ can attract fluorine atoms under some conditions. When the fluorocarbon bond is connected with aromatic or alkenyl electron rich groups, the reaction activity will be improved, or the stability of the fluorocarbon bond at the defect is relatively low. At this time, MnO_3^+ can attract the fluorine atoms in the fluorocarbon bond, and then the fluorocarbon bond will be broken, forming the excessive product MnO_3-F. Under acidic conditions, fluorine atoms can attract hydrogen ions in the acid and form HF. Meanwhile, the carbon with lost fluorine atoms has positive formal charge and can combine with hydroxyl ionized by water to form alcohol. In this process, MnO_3^+ acts as a catalyst. At the same time, the unsaturated carbon bonds of aryl or alkenyl groups are also oxidized by MnO_3^+. When these fluorocarbon bonds linked to aryl or alkenyl groups are completed, the remaining saturated fluorocarbon bonds are difficult to be catalyzed by MnO_3^+ due to their weak reactivity.

The reaction of fluorocarbon bonds catalyzed by MnO_3^+ and the oxidation of unsaturated carbon bond may take place simultaneously. According to Table 2, with the increase of $KMnO_4$, unsaturated carbon-carbon bonds are first oxidized to carbon-oxygen bond, then oxidized to C=O bond, and finally oxidized to the carboxyl group, and the content of fluorocarbon bond will decrease due to the catalytic reaction of fluorocarbon bond. Although $KMnO_4$ is more, the carbon-oxygen bond content of OFG42-3 is lower than that of OFG42-4, and the fluorocarbon bond is on the contrary. The possible reason is the relative deficiency of sulphuric acid, which reduces oxidicability. When the amount of sulphuric acid in OFG42-3 is enough, MnO_3^+ tends to oxidize the carbon-carbon double bond first, and then catalyze the activated fluorocarbon bond reaction. Part of sp^2 C=C in OFG42-1 is not oxidized. It is speculated that there may be too many oxygen-containing groups, which hinder the oxidation reaction, or the oxygen-containing groups may recover sp^2 C=C bond under some conditions, and then reach a certain balance with the oxidation process.

With the increase in $KMnO_4$ content, the fluorocarbons bond content in OFG42 decreased gradually, but the F ion content of the corresponding residual product doesn't increase significantly. The reason is that in acid solution, F ion is easy to combine with hydrogen ion to form HF. With the increase in HF content, it will gradually overflow in the form of gas, resulting in the loss of F element. In addition, the generated HF may form intermolecular hydrogen bond with fluorine atom through hydrogen bond, thus promoting the departure of F atom and accelerating the reaction process. In general, the possible reactions in this process are shown in Fig. 15: the catalytic reaction of fluorocarbon bond connected to unsaturated carbon bond, the oxidation of unsaturated carbon carbon bond, the catalytic reaction of fluorocarbon bond on saturated carbon, the oxidation of carbon oxygen single bond, etc. From the reduced fluorocarbon bond content and increased carbon oxygen bond in OFG42-4, it can be considered that the catalytic reaction of alkenyl or aryl fluorocarbon bond and the oxidation reaction of unsaturated carbon carbon bond will take place simultaneously. When the amount of $KMnO_4$ is further increased, catalytic reaction and oxidation reaction will be further deepened. Finally, when the mass ratio is more than 2, the reaction of fluorocarbon bond has stopped, only part of carbon oxygen bond is further oxidized to carbonyl, and the oxidation of carbon carbon double bond is accompanied by dehydration and condensation of carbon oxygen single bond to form carbon carbon double bond, reaching a dynamic balance. The residual fluorocarbon bond should be the fluorocarbon bond on the relatively isolated saturated carbon, and the reaction activity can't be catalyzed, so it has been retained. In order to verify this, the high fluorine content FGi is also used for experiments, and the results are shown in the supplementary information. It can be seen that FGi with high fluorine content is difficult to be oxidized due to its few unsaturated carbon bonds, and its oxygen content is very low, but there are still F ions in the remaining products, indicating that some of the fluorocarbon bonds connected with the unsaturated carbon bonds are activated and then react, and other saturated fluorocarbon bonds are difficult to be activated.

Because of the existence of large amount of graphite phase in FGi 42wt%, like the preparation of graphene oxide by Hummers method, it is easy to oxidize and break into fragments for FGi. The main

chemical changes and the influence on the structure include [33]: manganese cyclic ester compound makes the internal C=C bond break to form two carbonyls; two carboxylic acids are formed by C=C bond oxidation at the edge; one carboxylic acid and one ketone are formed by ketone oxidation fracture at the edge; two hydroxyl groups are formed by acid catalyzed hydrolysis of epoxy group. Adding water will further cause fragmentation. This explains the source of OFG fragments. In addition to the reaction of fluorocarbon bond, the continuous separation of OFG fragments from the carbon skeleton is also a reason for the continuous decrease of F content in OFG. This can not only explain the decrease of OFG size, but also explain that there is only carboxyl group in OFG and no ketone group, because these OFGs are originally produced by oxidative fracture, whose oxygen-containing groups are concentrated at the edge, and excessive $KMnO_4$ will fully oxidize the ketone group at the edge to carboxyl group. From OFG42-1 to OFG42-4, all own S element, but no K element, because there exists covalent sulfate [34–35], which hydrolyzes very slowly in acid solution, and the C-F bond nearby may make it difficult for water molecules to approach.

4 Conclusion

By adjusting the mass ratio of $KMnO_4$/ FGi 42 wt%, FGi 42 wt% can be oxidized in different degrees. With the increase in mass ratio, the effect of oxidization becomes better, which makes the oxygen content increase greatly and the fluorine content decrease obviously. When the mass ratio is greater than 2, FGi is oxidized completely, and the F content is lower than 6 at%; when the mass ratio is 1, OFG has higher fluorine and oxygen content with 21.6 at% F content and 20.3 at% O content respectively. OFG obtained by oxidation has a thin layered structure.

In short, the main mechanism of $KMnO_4$ modification is that MnO_3^+ with Lewis acid property can catalyze the activation of the fluorocarbon bond connected with the unsaturated carbon bond, and then the fluorocarbon bond breaks to form a new ion bond. At the same time, the unsaturated carbon bond is oxidized, resulting in the increase in carbon oxygen bond content and the generation of some OFG nano fragments. In the oxidation of FGi 42 wt% by $KMnO_4$, with the increase in $KMnO_4$ content, the fluorocarbon bond reaction will be gradually catalyzed while the unsaturated carbon bond is oxidized, and the catalytic reaction will be in order according to the fluorocarbon bond activity, finally there are still some fluorocarbon bonds with weak activity. Sulphuric acid+ $KMnO_4$ oxidation system can catalyze most of the fluorocarbon bond reactions, but can’t make the isolated fluorocarbon bond reactions.

Declarations

Acknowledgements

This research was supported by Natural Science Basic Research Program of Shaanxi (Program No.2020JQ-488).

Declaration of interests

The authors declare that they have no known competing financial interests or personal relationships that could have appeared to influence the work reported in this paper.

References

1. Akshay Mathkar, T. N. Narayanan, Lawrence B. Alemany, Paris Cox, Patrick Nguyen, Guanhui Gao et al 2013 *Part. Part. Syst. Charact.***30** 266
2. Wang Zhaofeng, Wang Jinqing, Li Zhangpeng 2012 *Carbon***50** 5403
3. Kaiming Hou, Peiwei Gong, Jinqing Wang, Zhigang Yang, Limin Ma, Shengrong Yang 2015 *Tribol. Lett.***60** 1
4. Peiwei Gong, Zhaofeng Wang, Zengjie Fan, Wei Hong, Zhigang Yang, Jinqing Wang et al 2014 *Carbon***72** 176
5. T. Bharathidasan, Tharangattu N. Narayanan, S. Sathyanaryanan, S.S. Sreejakumari 2015 *Carbon***84** 207
6. Fan Li, Weili Wei, Die Gao, Zhining Xi 2017 *Anal. Methods***9** 6645
7. Yeon Hoo Kim, Ji Soo Park, You-Rim Choi, Seo Yun Park, Seon Yong Lee, Woonbae Sohn et al 2017 *J. Mater. Chem. A***5** 19116
8. Antony Raj Thiruppathi, Boopathi Sidhureddy, Werden Keeler, Aicheng Chen 2017 *Electrochem. Commun.***76** 42
9. Sruthi Radhakrishnan, Parambath M. Sudeep, Jun Hyoung Park, Cristiano F. Woellner, Kierstein Maladonado, Douglas S. Galvao et al 2017 *Part. Part. Syst. Charact.***34** 1700245
10. Peiwei Gong, Shuaijie Ji, Jinqing Wang, Dujuan Dai, Fei Wang, Meng Tian et al 2018 *Chem. Eng. J.***348** 438
11. Shijing Yan, Jianqing Zhao, Yanchao Yuan, Shumei Liu, Zhenxun Huang, Zhigeng Chen et al 2013 *RSC Adv.***3** 21869
12. Xiao Chen, Haohao Huang, Xia Shu, Shumei Liu, Jianqing Zhao 2017 *RSC Adv.***7** 1956
13. P. M. Sudeep, J. Taha-Tijerina, P. M. Ajayan, T. N. Narayananc, M. R. Anantharaman 2014 *RSC Adv.***4** 24887
14. Peiwei Gong, Zhigang Yang, Wei Hong, Zhaofeng Wang, Kaiming Hou, Jinqing Wang et al 2015 *Carbon***83** 152
15. Yang X, Jia X, Ji X 2015 *RSC Adv.***5** 9337
16. Jankovský O, Šimek P, Sedmidubský D, Stanislava Matějková, Zbyněk Janoušek, Filip Šembera et al 2014 *RSC Adv.***4** 1378
17. Mazánek V, Jankovský O, Luxa J, David Sedmidubský, Zbyněk Janoušek, Filip Šembera et al 2015 *Nanoscale***7** 13646
18. Ji Chen, Yingru Li, Liang Huang, Chun Li, Gaoquan Shi 2015 *Carbon***81** 826

19. Fu-Gang Zhao, Gang Zhao, Xin-Hua Liu, Cong-Wu Ge, Jin-Tu Wang, Bai-Li Li et al 2014 *J. Mater. Chem. A***2** 8782
20. Jan Plšek, Karolina Anna Drogowska, Václav Valeš, Johan Ek Weis, Martin Kalbac 2016 *Chem.-Eur. J.***22** 8990
21. Demetrios D.Chronopoulos, Aristides Bakandritsos, Martin Pykal, Radek Zbořil, Michal Otyepka 2017 *Appl. Mater. Today***9** 60
22. Cheng Zhang, Tao Tao, Wenjuan Yuan, Lei Zhang, Xiaoqin Zhang, Jun Yao et al 2017 *Anal. Chem.***89** 4566
23. Xuequan Zhang, Yiyu Feng, Dong Huang, Yu Li, Wei Feng 2010 *Carbon***48** 3236
24. Yu W, Yang Y, Graham N 2016 *Chem. Eng. J.***298** 234
25. Murch GE, Thorn RJ 1980 *J. Phys. Chem. Solids***41** 785
26. Morgan WE, Wazer JRV, Stec WJ 1973 *J. Am. Chem. Soc.***95** 751
27. Amii H, Uneyama K 2009 *Chem. Rev.***109** 2119
28. Kiplinger JL, Richmond TG, Osterberg CE 1994 *Chem. Rev.***94** 373
29. Storm MM, Johnsen RE, Norby P 2016 *J. Solid State Chem.***240** 49
30. Chunhu Chen, Shin Hu, Jyunfu Shih, Changying Yang, Yunwen Luo, Renhuai Jhang et al 2017 *Sci. Rep.***7** 3908
31. Stahl T, Klare HFT, Oestreich M 2013 *ACS Catal.***3** 1578
32. Scott VJ, Celenligil-Cetin R, Ozerov OV 2005 *J. Am. Chem. Soc.***127** 2852
33. Jong Hun Kang, Taehoon Kim, Jaeyoo Choi, Jisoo Park, Yern Seung Kim, Mi Se Chang et al 2016 *Chem. Mat.***28** 756
34. Dimiev AM, Tour JM 2014 *ACS Nano***8** 3060
35. Siegfried Eigler, Christoph Dotzer, Ferdinand Hof, Walter Bauer, Andreas Hirsch 2013 *Chem.-Eur. J.***19** 9490

Figures

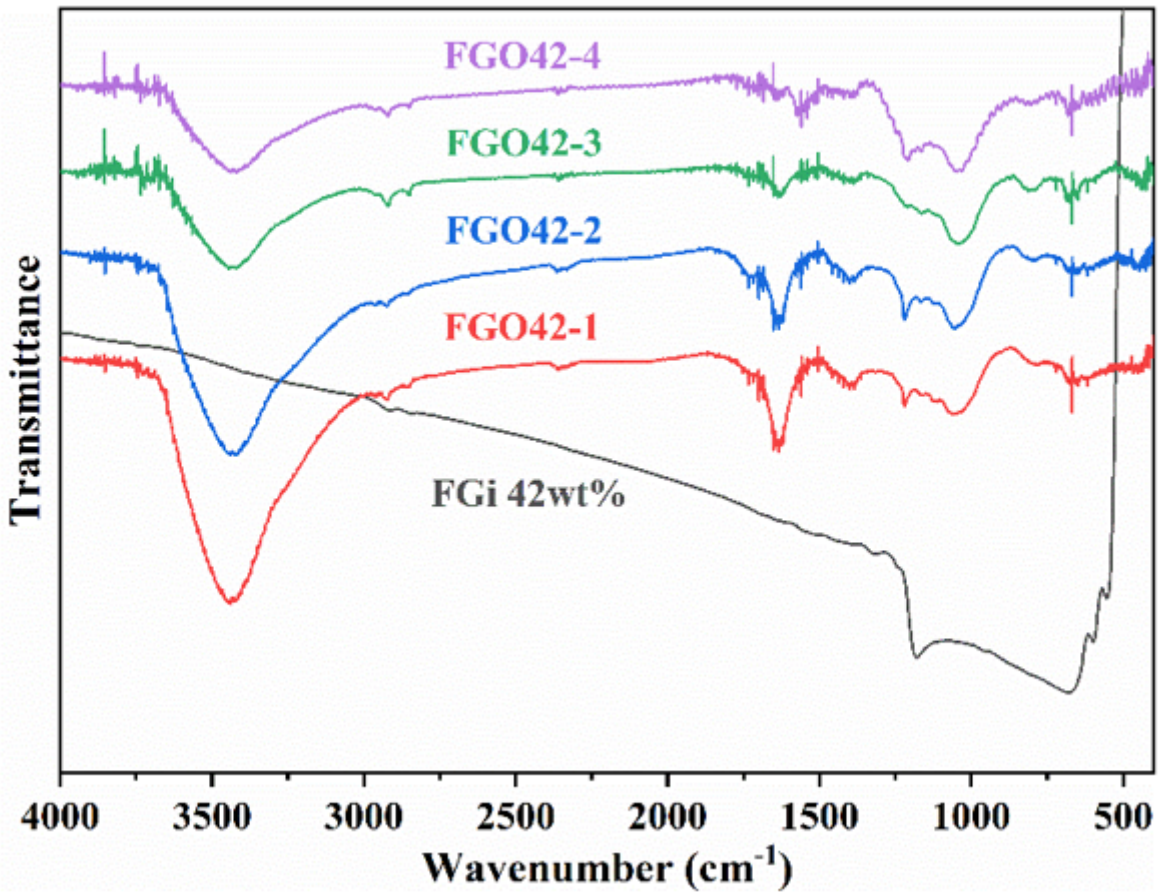

Figure 1

FT-IR spectra of OFG42-1(1:8), OFG42-2(1:2), OFG42-3(2:3) and OFG42-4(1:3)

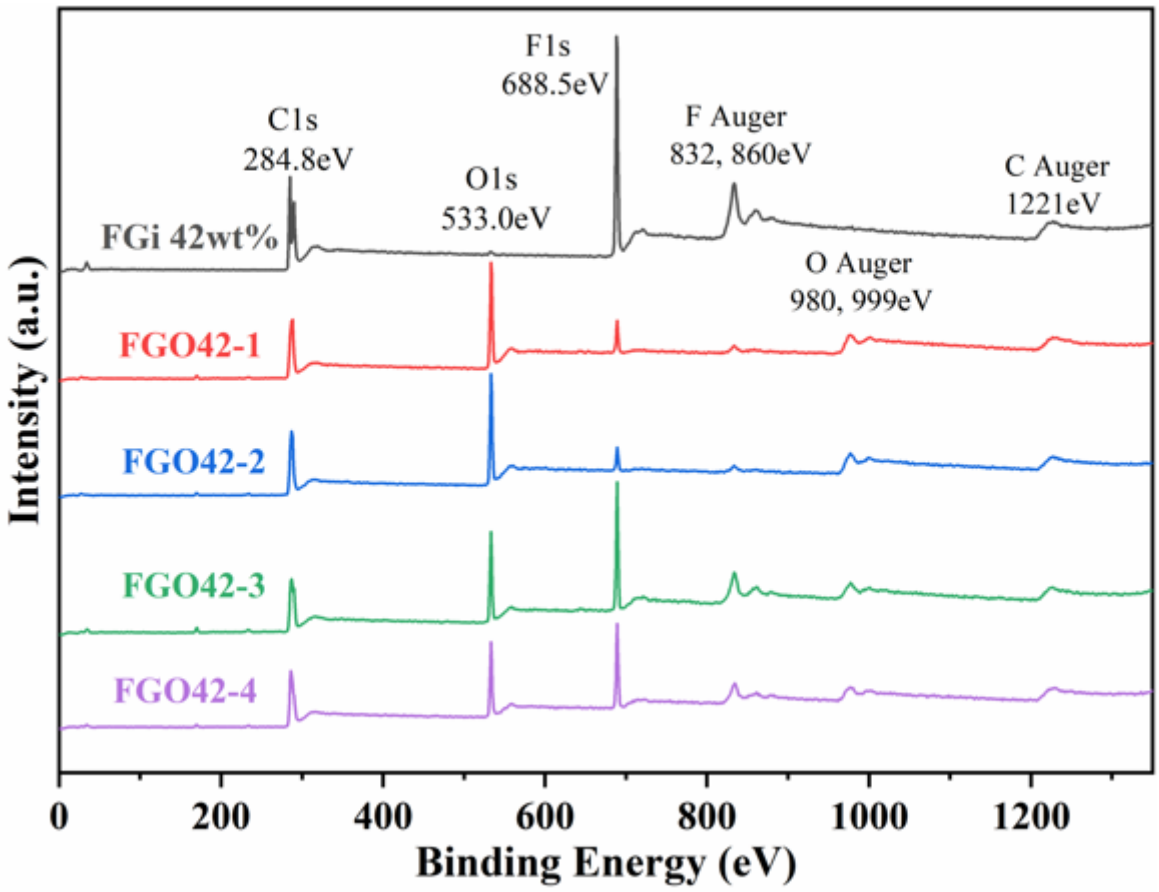

Figure 2

XPS spectra of OFG42-1, OFG42-2, OFG42-3 and OFG42-4

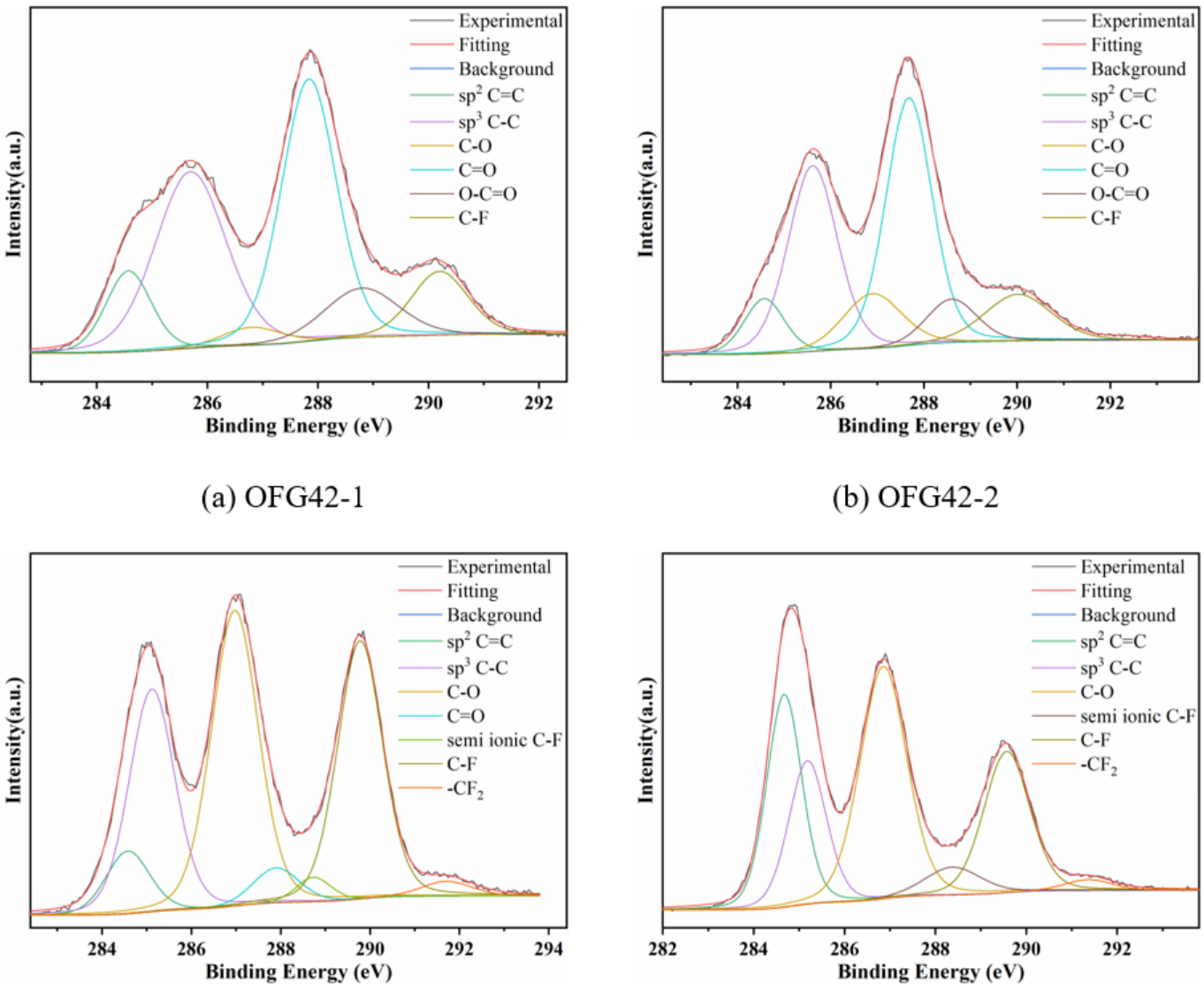

Figure 3

High-resolution C1s spectra of OFG42-1, OFG42-2, OFG42-3 and OFG42-4

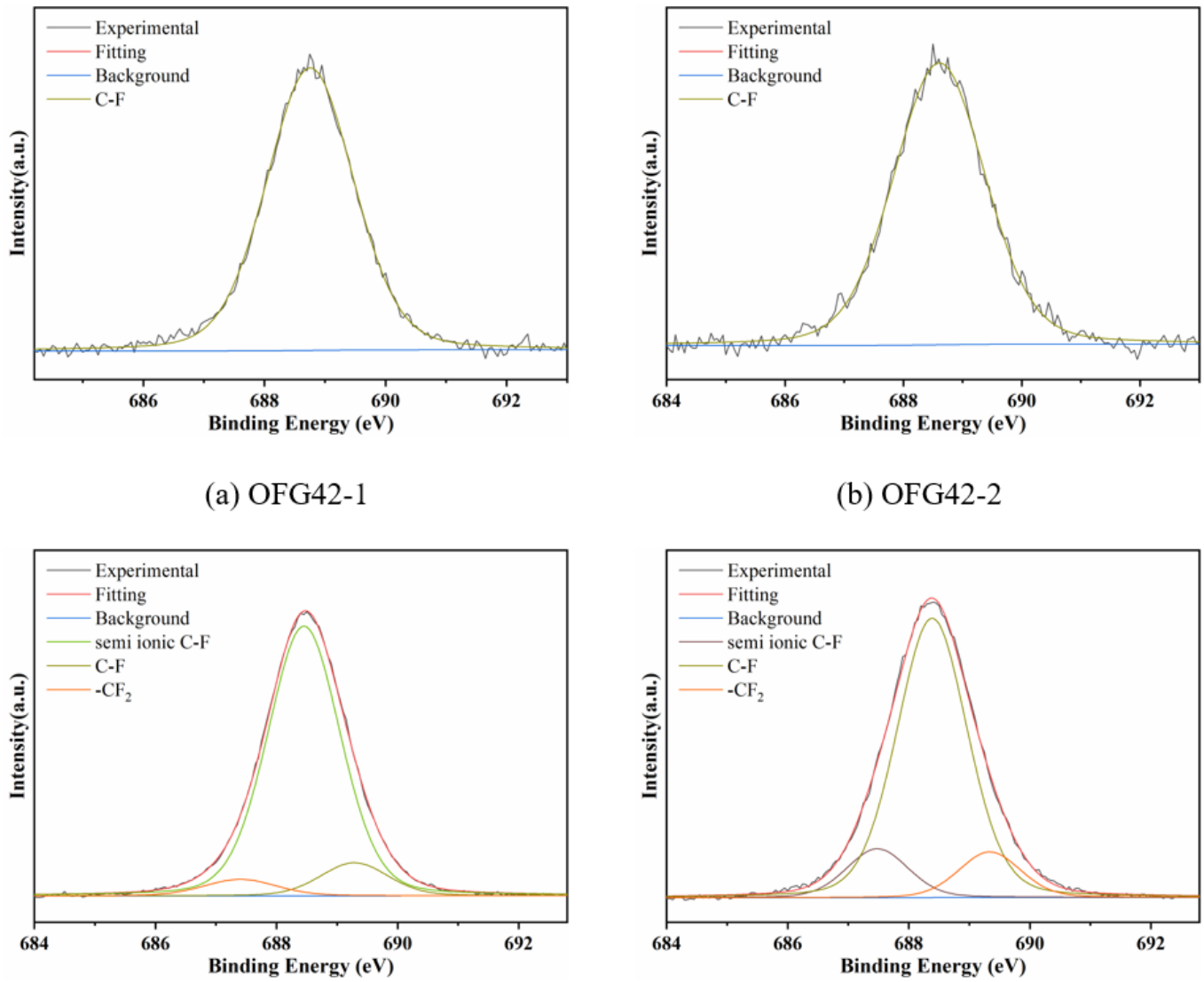

Figure 4

High-resolution F1s spectra of OFG42-1, OFG42-2, OFG42-3 and OFG42-4

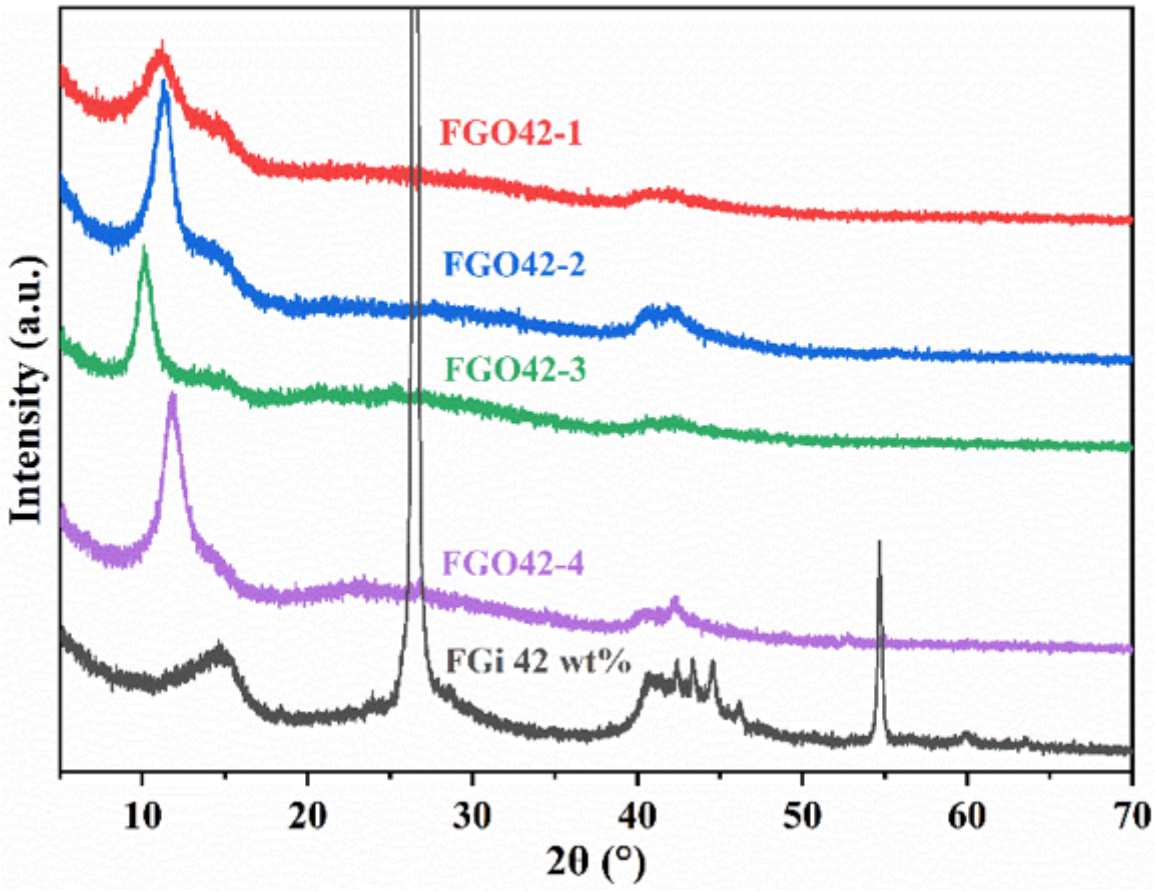

Figure 5

XRD spectra of OFG42-1, OFG42-2, OFG42-3 and OFG42-4

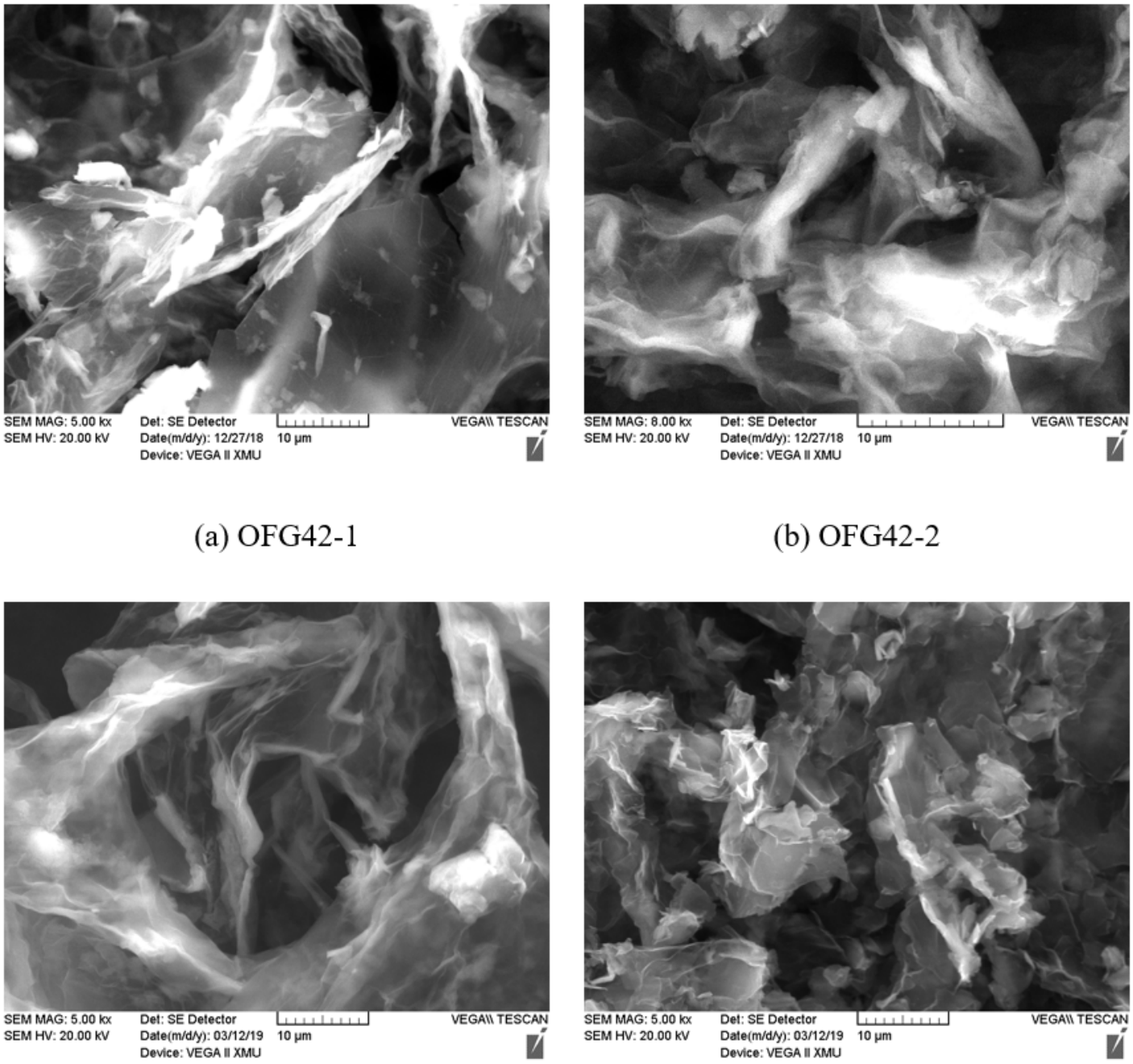

Figure 6

SEM images of OFG42-1, OFG42-2, OFG42-3 and OFG42-4

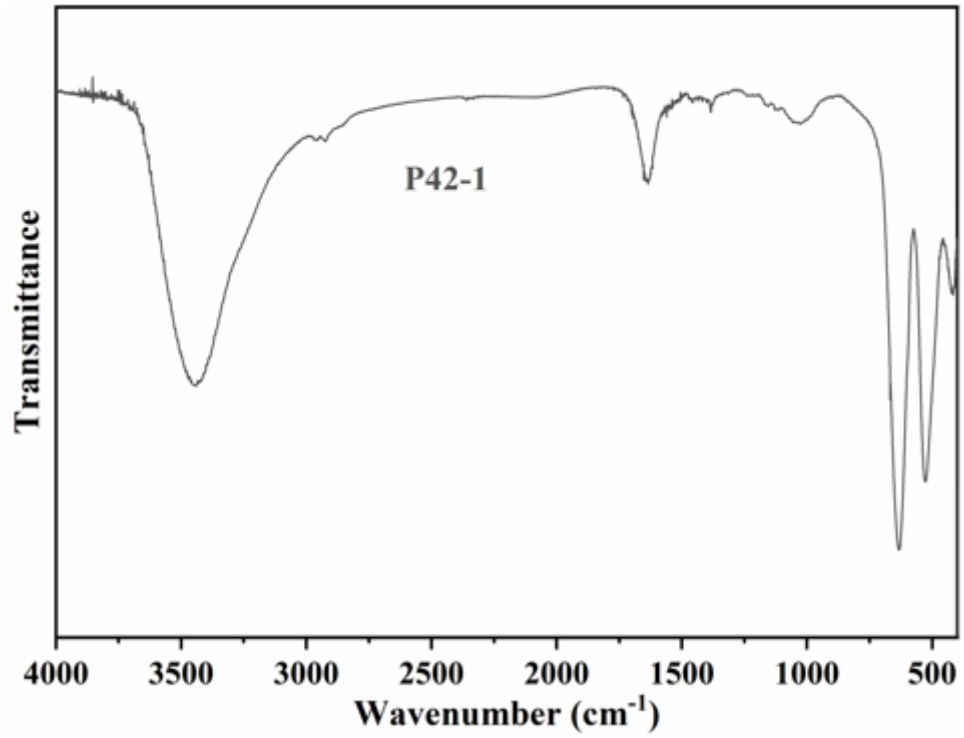

Figure 7

FT-IR spectra of P42-1

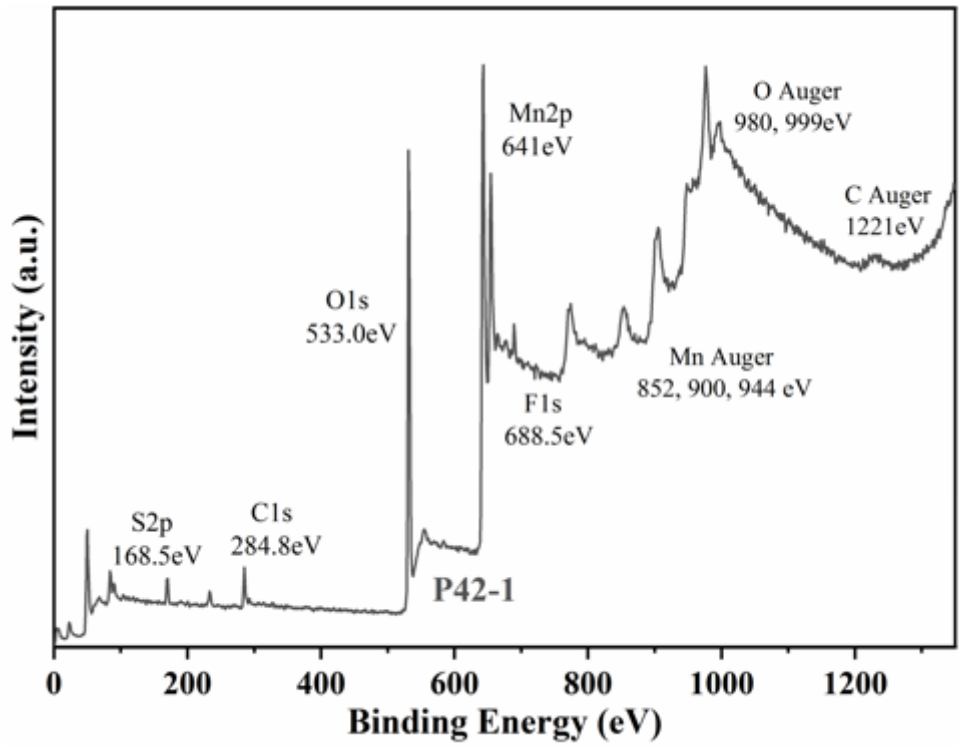

Figure 8

XPS spectra of P42-1

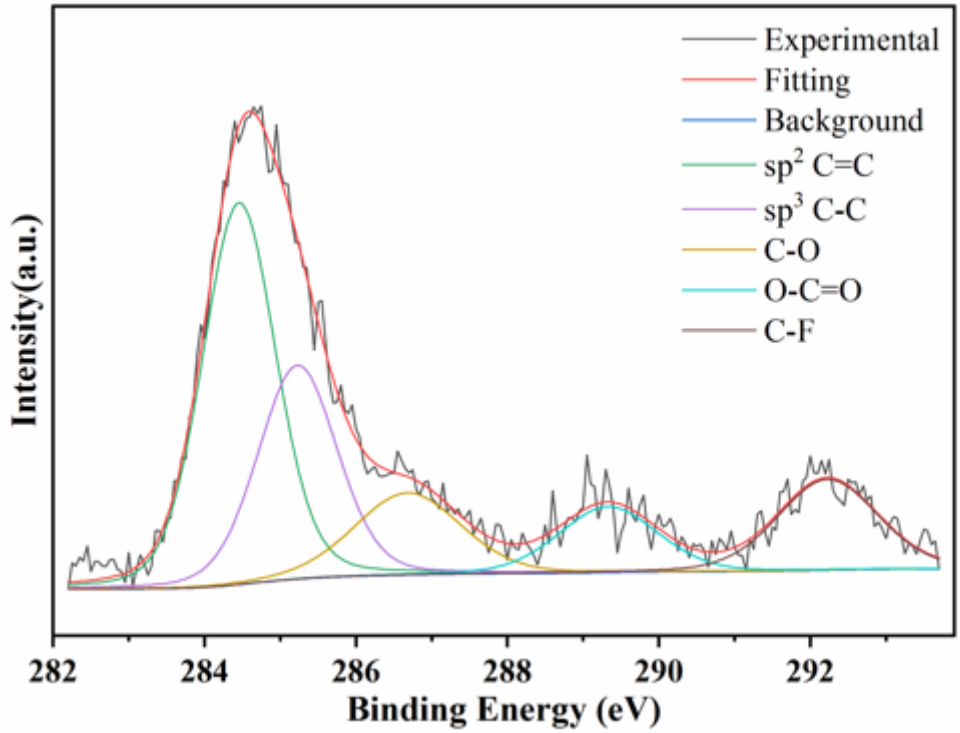

Figure 9

High-resolution C1s spectra of P42-1

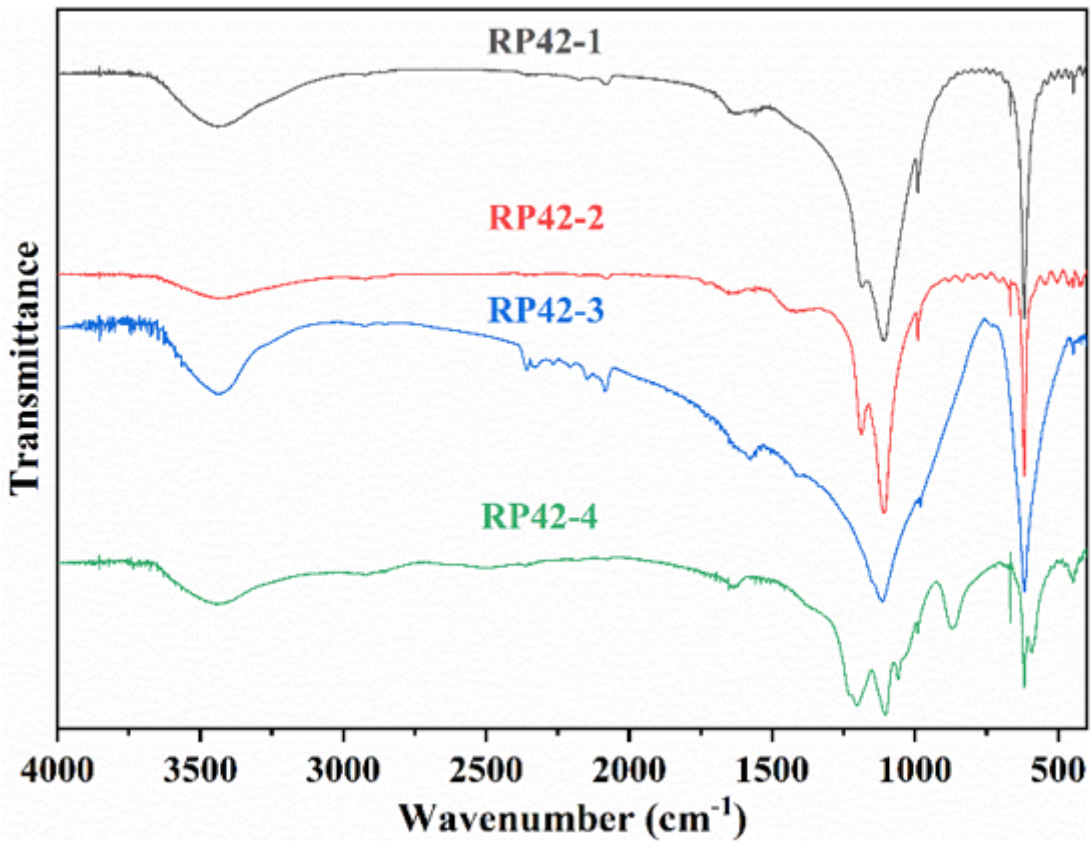

Figure 10

FT-IR spectra of RP42-1, RP42-2, RP42-3 and RP42-4

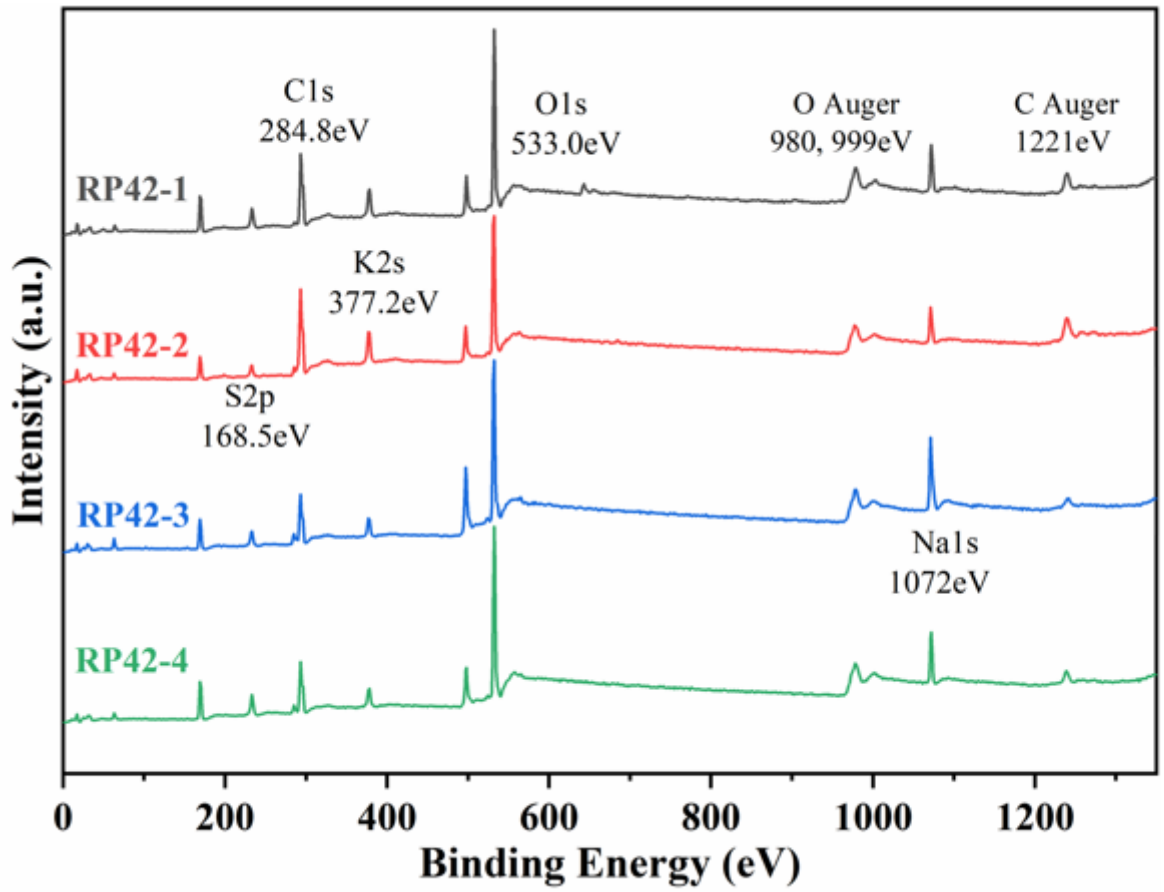

Figure 11

XPS spectra of RP42-1, RP42-2, RP42-3 and RP42-4

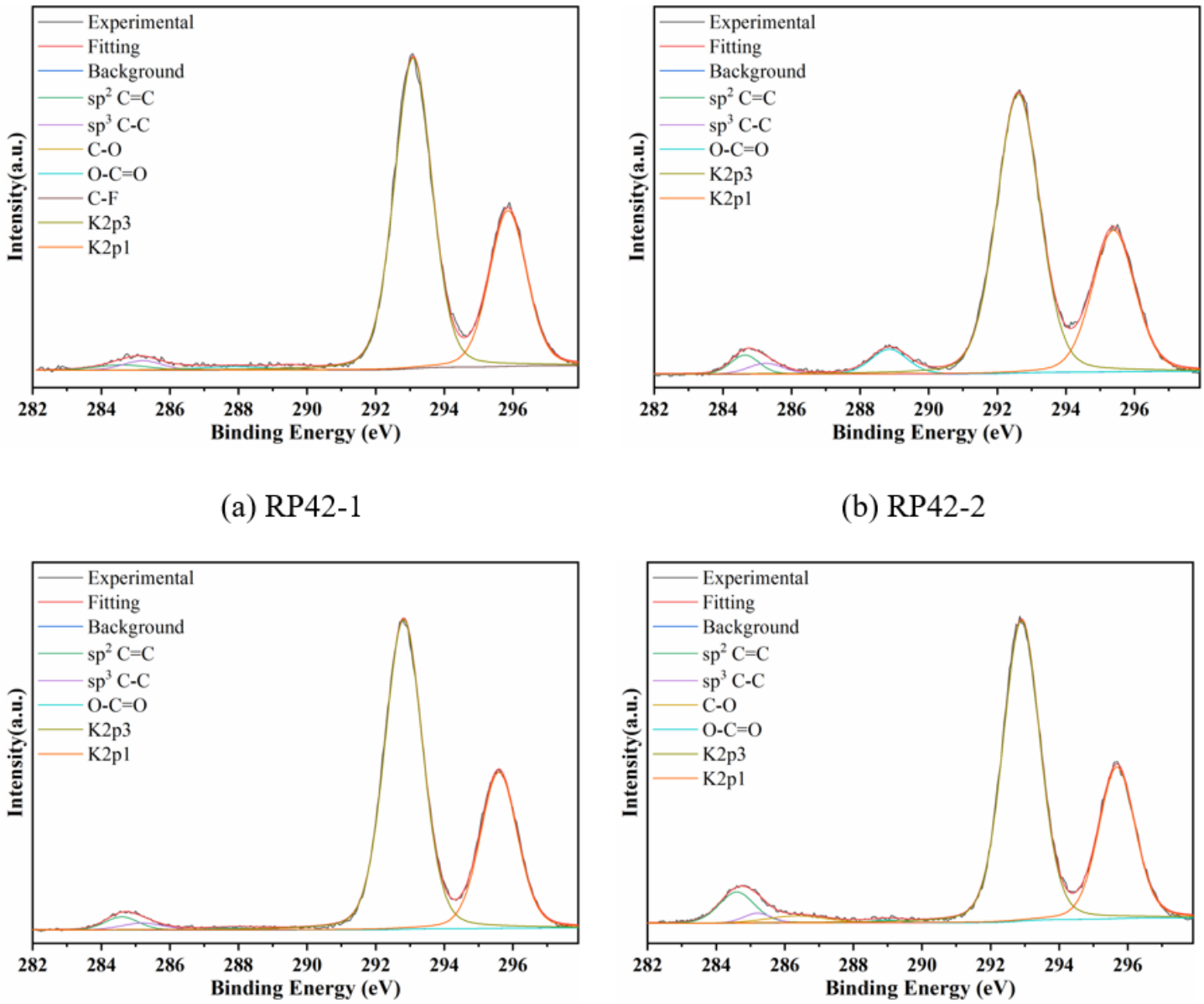

Figure 12

High-resolution C1s spectra of RP42-1, RP42-2, RP42-3 and RP42-4

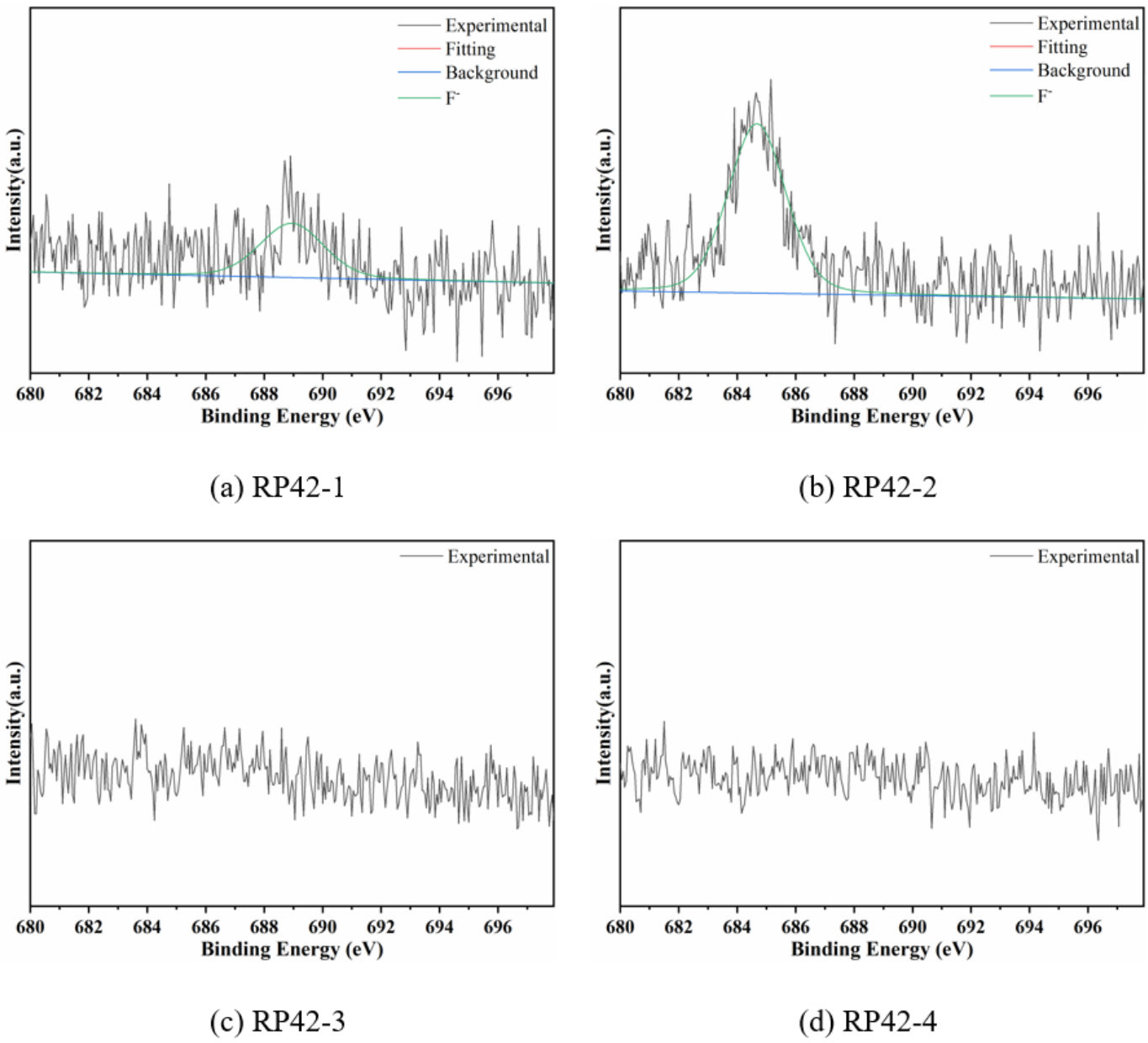

Figure 13

High-resolution F1s spectra of RP42-1, RP42-2, RP42-3 and RP42-4

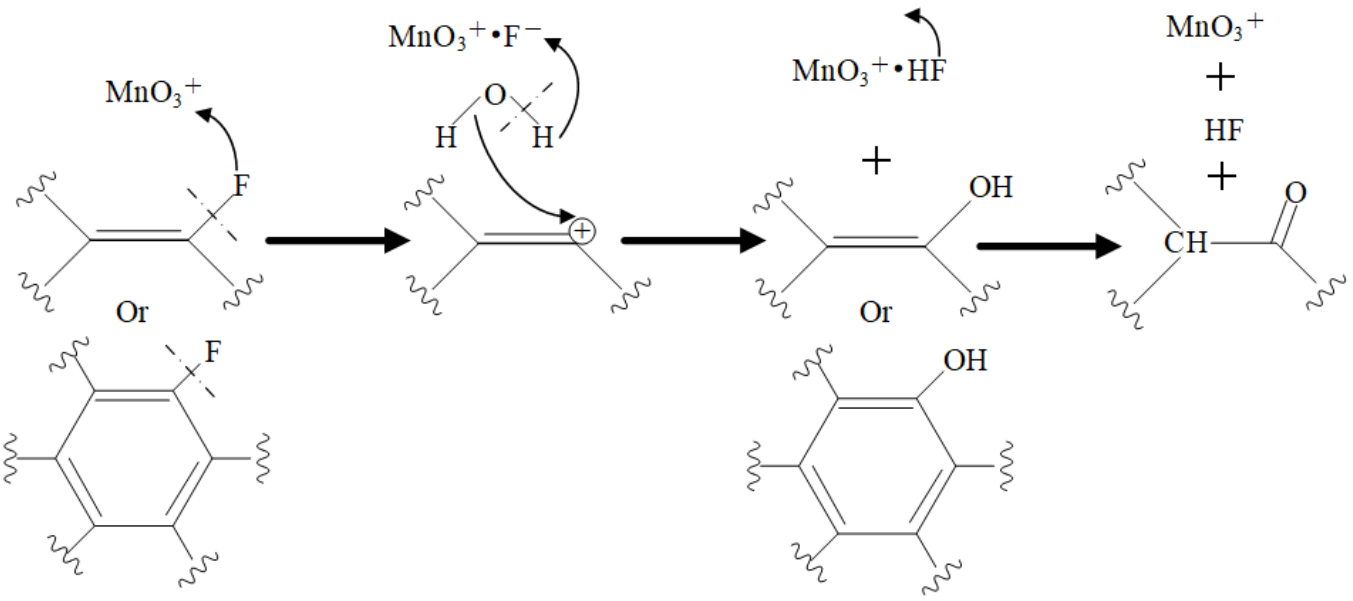

Figure 14

Proposed reaction mechanism of fluorocarbon bond activation

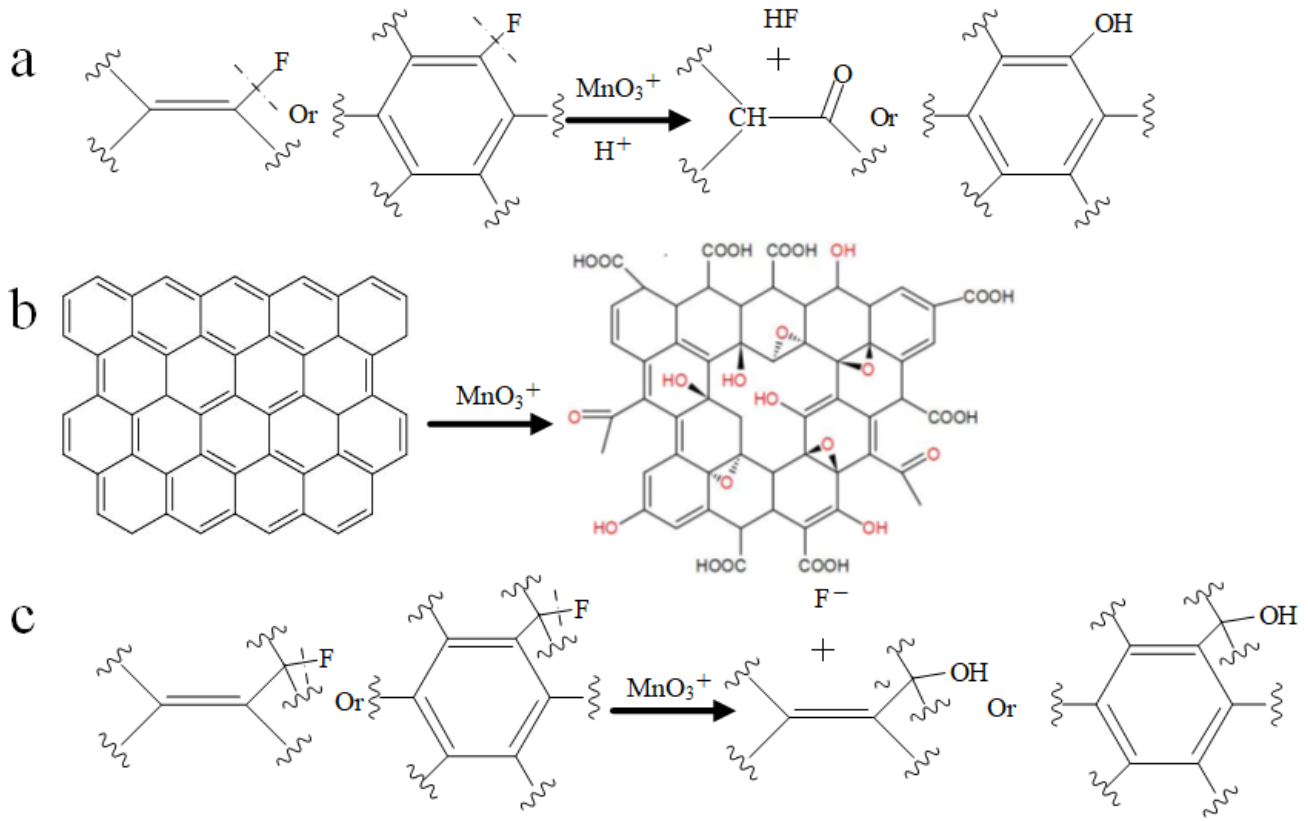

Figure 15

Proposed reaction mechanism of FGi 42 wt% modification by KMnO4

Supplementary Files

This is a list of supplementary files associated with this preprint. Click to download.

- SupportingInformation.docx